Conference paper

Jan Šubrt*, Eva Pližingrová, Monika Palkovská, Jaroslav Boháček, Mariana Klementová, Jaroslav Kupčík, Petr Bezdička and Helena Sovová

Titania aerogels with tailored nano and microstructure: comparison of lyophilization and supercritical drying

DOI 10.1515/pac-2016-1031

Abstract: Structure and phase composition of titania aerogels can be substantially influenced simply by the process of drying their parent water colloid suspensions prepared by the reaction of hydrogen peroxide with suspension of precipitates obtained by neutralization of solution of titanyl sulfate with ammonia. Two methods of drying are compared: (1) lyophilization of fast frozen material immersed in liquid nitrogen, and (2) critical point drying using supercritical CO_2 under high pressure. Both methods of drying lead to yellow titanium peroxide aerogels consisting of nanometer-sized blocks. While lyophilization leads to foils consisting of nano-sized crystalline nuclei of peroxo-polytitanic acid dispersed in predominantly amorphous material, the critical point drying provides rather bulk highly porous composite consisting of randomly oriented flat nanoparticles (5–10 nm) composed of crystalline anatase and amorphous peroxo-polytitanic acid.

Keywords: aerogels; critical point drying; lyophilization; peroxo-polytitanic acid; SSC-2016; titanium dioxide.

Introduction

The wet-chemical approach is a very important one among the different methods to prepare new nanostructured materials. A lot of different wet chemical approaches, so-called bottom-up fabrication methods, of nanostructured solids of different sizes, shapes and material compositions are known, both in polar and non-polar solvents [1]. It has been published recently [2, 3] that a network of thin platelets building up the gel network can be prepared by freezing aqueous colloids *in situ* and subsequent freeze drying (lyophilization) or by critical point drying. The advantage of this strategy is its suitability for various nanoparticle systems, since there is no chemical selectivity. At the best case, the volume and shape of the resulting aerogel is the same as the volume and shape of the initial hydrogel.

Hydrogels are usually considered as aqueous jelly-like material, in properties ranging from soft and weak to hard and tough. The continuity of the liquid permeating jellies was demonstrated by diffusion, syneresis, and ultrafiltration, and the fact that the liquid may be replaced by other liquids of very diverse character

Article note: A collection of invited papers based on presentations at the 12th Conference on Solid State Chemistry (SSC-2016), Prague, Czech Republic, 18–23 September 2016.

***Corresponding author: Jan Šubrt,** Institute of Inorganic Chemistry of the CAS, v.v.i., CZ-250 68 Husinec-Řež, Czech Republic, e-mail: subrt@iic.cas.cz
Eva Pližingrová, Jaroslav Boháček, Mariana Klementová, Jaroslav Kupčík and Petr Bezdička: Institute of Inorganic Chemistry of the CAS, v.v.i., CZ-250 68 Husinec-Řež, Czech Republic
Monika Palkovská: Institute of Inorganic Chemistry of the CAS, v.v.i., CZ-250 68 Husinec-Řež, Czech Republic; and Department of Chemistry, Faculty of Science, University of Ostrava, Ostrava, CZ-701 30, Czech Republic
Helena Sovová: Institute of Chemical Process Fundamentals of the CAS, v.v.i., CZ-165 02 Prague, Czech Republic

indicates clearly that the gel structure may be independent of the liquid in which it is bathed. The attempt to remove the liquid by evaporation usually results in extensive shrinkage and possible structural damage of the material [4, 5].

To avoid this, the sample can be dried via two possible alternate paths from the liquid phase to the gas phase without crossing the liquid–gas boundary on the phase diagram. In freeze drying, solutions are frozen in a cold bath and then the frozen solvents are removed via sublimation under vacuum, leading to formation of porous structures. Pore size, pore volume and pore morphology are dependent on variables such as freeze temperature, solution concentration, nature of solvent and solute, and the control of the freezing direction [6]. Supercritical drying, on the other hand, proceeds at high temperature and high pressure above the critical point. This route from liquid to gas does not cross any phase boundary, instead passing through the supercritical region, where the distinction between gas and liquid ceases to apply.

Nanostructured titania both in the crystalline form of anatase and rutile represents important material widely used as catalysts, pigments, photocatalysts, components of batteries, and other technically important materials. However, except of classical sol-gel processes based on hydrolysis of titanium alkoxides, purely aqueous processes are rather rare in synthesis of such material despite the fact that use of water as solvent is clearly the most advantageous from both economic and ecological point of view. We successfully applied lyophilization for synthesis of highly photoactive 2D titanium dioxide nanostructures prepared from aqueous colloids of peroxo-polytitanic acid. Reaction of hydrogen peroxide with suspension of thoroughly washed precipitates obtained by neutralization of aqueous solution of titanyl sulphate with aqueous ammonia leads to transparent yellow colloid suspension. In this way prepared colloid suspension is a two phase system in which, beyond the water phase, also a liquid hydrated peroxo-polytitanic acid component is present [3]. During time the viscosity of the originally fluid liquid increases and the material transforms into viscous hydrogel as a result of polymerization processes of planar titanium peroxo-complexes [7, 8].

In this work, yellow colloid suspensions of peroxo-polytitanic acid were dehydrated using lyophilization of fast frozen materials obtained by immersion in liquid nitrogen as well as by drying process using supercritical CO_2. Structural and morphological investigations have shown some common features as well as some differences between products of drying resulting from different mechanisms of arrangement of nanoparticles during the drying processes.

Materials and methods

Chemicals

As a titanium precursor, titanium (IV) oxysulfate ($TiOSO_4 \cdot nH_2O$, technical grade purity, min. 29 % Ti as TiO_2, Sigma-Aldrich) was used. Aqueous solution of ammonia (NH_3, solution purum p.a., 25–29 %, Penta) served for precipitation, and subsequent pH reduction was carried out by adding of hydrogen peroxide (H_2O_2, solution purum p.a., 30 %, Penta). Methanol (CH_3OH, solution purum p.a., Penta) was used for water exchange during the process of critical point drying.

Sample preparation and drying methods

Titania colloid suspensions were prepared from $TiOSO_4 \cdot nH_2O$ according to the following procedure [3, 9]: 4.80 g of titanium (IV) oxysulfate was stirred into 150 mL of distilled water at 35 °C, and the solution was cooled down to 0 °C. Then ammonia was added to the cold solution until pH = 8, and a white precipitate was formed. The precipitate was filtered off, washed and transferred into a beaker, and resuspended in 350 mL of distilled water. The pH value of the resulting suspension was reduced to pH = 3–4 by adding 20 mL of hydrogen peroxide, and the suspension turned cloudy yellow. After 1 h of stirring the suspension became

transparent yellow. Before drying, the suspension was left for a couple of days at room temperature (RT). Titania aerogels were prepared from the yellow suspension by lyophilization and critical point drying.

Lyophilization (freeze drying)

The suspension was dripped into liquid nitrogen; the frozen material was then transferred to a freeze drier and lyophilized (VirTis Benchtop K, Cole Parmer, UK) at temperature of the condenser – 56 °C and final pressure of 1 Pa until the full removal of water. The lyophilized titania aerogel is labeled as LYO.

Critical point drying (supercritical drying)

Forty gram of yellow colloid suspension was placed on a layer of glass beads and glass wool into a 150 mL high-pressure column with the inner diameter of 30 mm and a tempering jacket. The column was immersed in a heated water bath at 40 °C. The suspension was repeatedly washed with 150 mL of methanol. First, the column was filled with methanol using a syringe. (A gradual reduction in the volume of the colloid suspension in methanol was observed in a view cell where a preliminary experiment was carried out with 1 g of suspension at the same conditions.) After 3 h, the methanol phase was carefully removed and replaced with pure methanol. After another 3 h the process was repeated and the suspension was left in the bath overnight. Then methanol phase was again removed from the column, which was connected to a high-pressure pump and filled with CO_2 to a pressure of 9 MPa. The column was left for 30 min to stabilize the pressure and temperature, and then the flow of CO_2 was set to 1.7 g min^{-1}. The sample was dried at 40 °C and pressure of 9 MPa under the flow of CO_2 for 5 h. The flow of CO_2 was stopped after 2 h and the column was immersed in water at 60 °C and depressurized slowly to avoid excessive cooling, which would be accompanied by condensation of CO_2. The details of the equipment were given recently by Sajfrtova et al. [10]. The critical point dried titania aerogel is labeled as CPD.

Characterization methods

Electron microscopy

Scanning electron microscopy (SEM): Morphology of samples was revealed by the scanning electron microscope Philips CP XL 30 equipped with energy dispersive X-ray (EDX) detector. Measurements were carried out in a high vacuum mode, and accelerating voltage of 10 kV for studying of LYO sample and 30 kV for CPD sample. For some measurements using secondary electrons (SE), the samples were coated with a thin (60 nm) conductive Au-10 % Pd alloy layer.

Transmission electron microscopy (TEM): Transmission electron micrographs were obtained using a JEOL JEM 3010 microscope operated at accelerating voltage of 300 kV (LaB_6 cathode, point resolution 1.7 Å) with a Gatan slow-scan CCD camera (resolution 1024 × 1024 pixels) using the Digital Micrograph software package. Electron diffraction patterns were evaluated using the Process Diffraction software package [11]. The samples for TEM were prepared using grinding and dispersing the powder in propyl alcohol. A drop of dilute suspension was placed on a holey-carbon-coated Cu grid and let dry by evaporation at ambient temperature.

In situ high temperature X-Ray powder diffraction (HT XRD)

In situ high temperature diffraction patterns were collected with a PANalytical X'Pert PRO diffractometer equipped with a conventional X-ray tube ($Co_{K\alpha}$ radiation, 40 kV, 30 mA, line focus) and a multichannel detector X'Celerator with an anti-scatter shield. For experiments at elevated temperature the high temperature chamber (HTK 16, Anton Paar, Graz, Austria) was used. X-ray patterns were measured from room temperature

to 1200 °C with a step of 25 °C in the range of 19 to 93° 2 θ (step of 0.0334° and 40 s counting per step yielding a scan of ca 12 min). In this case we used conventional Bragg–Brentano geometry with 0.04 rad Soller slit, 1° divergence slit, 2° anti-scatter slit, and 10 mm mask in the incident beam, 6.6 mm anti-scatter slit, 0.04 rad Soller slit and Fe beta-filter in the diffracted beam. Samples were ground in an agate mortar in a suspension with cyclohexane. The suspension was then placed on top of the Platinum heating element. After evaporation of solvent, thin layer of as prepared sample was ready for analysis.

Qualitative analysis was performed with HighScorePlus software package (PANalytical, The Netherlands, version 4.5.0), DiffracPlus software package (Bruker AXS, Germany, version 8.0) and JCPDS PDF-4 database [12]. For quantitative analysis of samples we used Diffrac-Plus Topas (Bruker AXS, Germany, version 4.2) with structural models based JCPDS PDF-4 database [12]. This program permits to estimate the weight fractions and crystallite sizes of crystalline phases by means of Rietveld refinement procedure.

Infrared spectroscopy

The Fourier transform infrared spectra of the samples were measured by Nicolet Nexus 670 FTIR spectrometer in the form of KBr pellets (1 mg of a sample added to 300 mg of dried KBr powder) in the region 4000–400 cm^{-1}. The measured data were evaluated using programs Omnic and Origin.

Raman spectroscopy

Raman spectra were recorded using a dispersive Raman Nicolet Almega XR instrument (excitation wavelength 473 nm, output 10 mW, spectral range 100–1300 cm^{-1}, resolution 6, 5–13 cm^{-1}). Software package Omnic 8.2.0.387 (Thermo Fishes Scientific, inc.,) was used for analysis of the measured data. The Raman spectra of anatase and rutile shown for comparison were taken from Nicodom spectra library [13].

Surface area and porosity

Specific surface area was determined by the B.E.T. method (Brunauer, Emmett, Teller) [14] using a Quantachrome Nova 4200e instrument. Nitrogen adsorption was carried out at – 196 °C. The pore size distributions (pore diameter and pore volume) were evaluated from the nitrogen desorption isotherm using the cylindrical pore model BJH (Barrett, Joyner, and Halenda) [15], t-method and DFT method (density functional theory). Before measurement, the LYO sample was outgassed for approx. 35 h at RT and the CPD sample for approx. 44 h at RT.

Thermal analysis

Thermogravimetry (TG) and differential thermal analysis (DTA) were performed with the apparatus SetSys Evolution (SETARAM). TA measurements of prepared samples were performed in a crucible made of α-Al_2O_3 in argon flow (60 mL min^{-1}) at atmospheric pressure in temperature range from RT to 800 °C with heating rate of 5 °C min^{-1}. The dried fine powders (20–25 mg) of LYO and CPD samples were measured.

Results and discussion

Samples of titania aerogels prepared by two different methods of drying, lyophilization and critical point drying, were prepared. Their morphology, microstructure, and phase composition were studied.

SEM micrographs of LYO and CPD titania aerogels are displayed in Fig. 1. While the lyophilized material consists of well-separated very thin foils, the CPD aerogel is rather bulk material, although also exhibits signs of lamellar structure (Fig. 1b2). This fact is probably related to planar structure of titanium peroxide complex described in literature earlier [3, 7, 16, 17]. Morphological difference between LYO and CPD samples is best seen from the micrographs taken at the highest magnification. While the lyophilized sample (Fig. 1a3) shows very thin foils with rather smooth surface, the CPD sample (Fig. 1b3) shows highly porous material consisting of randomly oriented very small, probably planar, units.

Morphology and phase composition at nanoscale was studied by TEM (Fig. 2). The LYO sample shows the typical foil morphology. The foils have lateral size of several tens of micrometers and thickness of only about 10 to 20 nm, and are composed of tightly packed grains. The SAED pattern displays weak broad circles corresponding to peroxo polytitanic acid (Pdf 47-0124) with a very small grain size of about 2 nm bordering on amorphous character. On the contrary, the CPD sample displays 3D nanoporous microstructure composed of flat nanoparticles about 5 to 10 nm in size and 2 nm thick. Most of the particles are composed of crystalline anatase, whereas others seem to be amorphous.

Such differences can be easily understood on the basis of recently published concept of formation of self-supported aerogels of nanoparticle building blocks by freezing and subsequent freeze-drying of colloidal nanoparticle suspensions [2]. Authors suppose, that during fast freezing of nanoparticle containing aqueous colloids, nanoparticles originally evenly distributed within the aqueous medium aggregate on the surface of ice grains. After full freezing and removal of ice due to the lyophilization process, the remaining nanoparticles form assembled aggregates shape and size of which depends on conditions of freezing as well as on properties of the initial nanoparticle units. It is clear that by fast freezing aqueous colloidal nanoparticle suspensions, which were as droplets injected directly into liquid nitrogen, and by subsequent freeze drying the frozen objects, highly porous and voluminous aerogels consisting solely of the respective material can be obtained.

The CPD dried material, on the other hand, is not affected by the effect of growing ice grains and the structure of aerogel is probably closer to the structure of the original aqueous colloid. Figure 1b3 shows highly porous surface of the CPD material consisting of small randomly oriented nano-sized units. The planar shape of these nanostructures was confirmed also by HRTEM. Figure 2a3 and b3 display clearly planar nanoparticles in both lyophilized and CPD dried samples, which are more densely packed in the lyophilized sample. This is in agreement with the above mentioned mechanism of lyophilization of the fast frozen colloids.

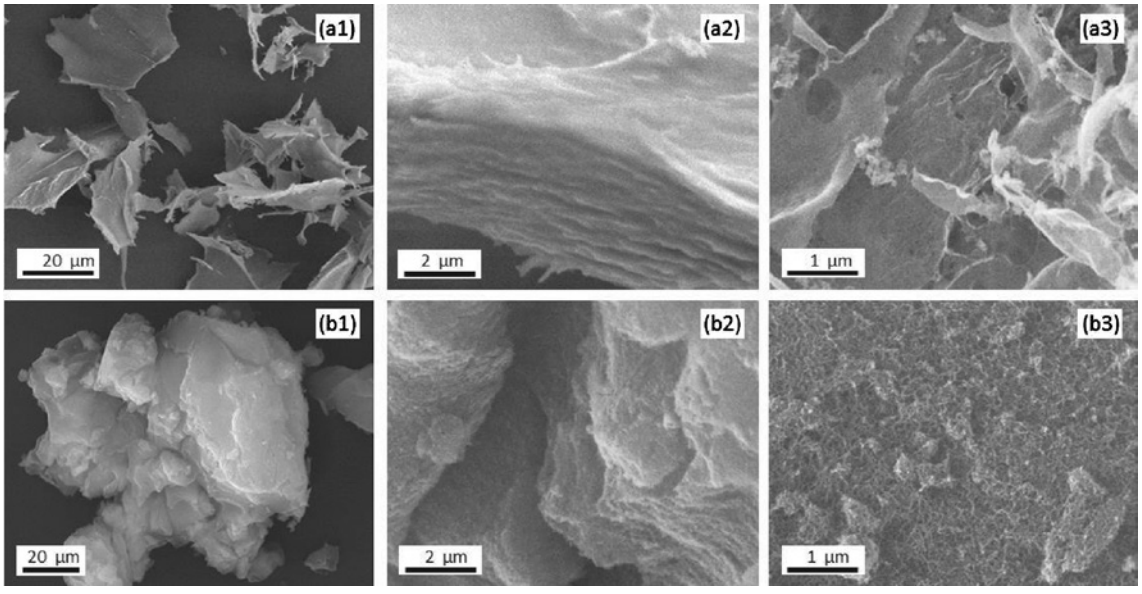

Fig. 1: SEM micrographs of lyophilized (a1–a3) and critical point dried (b1–b3) titania aerogels.

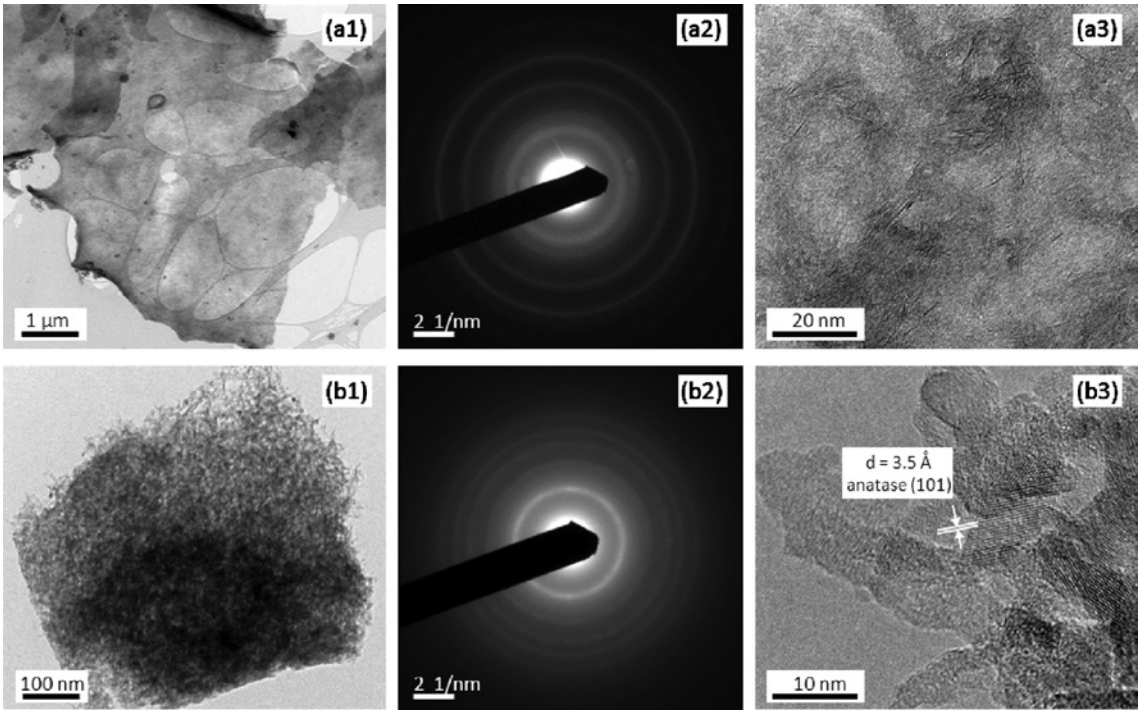

Fig. 2: TEM micrographs of lyophilized (a1–a3) and critical point dried (b1–b3) titania aerogels.

The drying procedure also affects the atomic structure of the titania aerogel and its behavior upon heating as is documented by the results of *in situ* HT XRD analysis shown in Fig. 3. The samples display significant differences. The lyophilized non-annealed material is amorphous up to 300 °C, when it suddenly crystallizes to anatase with sharp diffraction lines corresponding to crystallite size ranging from 25 nm at 400 °C to 40 nm at 900 °C, when the transition into rutile begins. The CPD sample, on the other hand, shows diffraction lines belonging to anatase even in the non-annealed sample. The lines are very broad corresponding to very fine crystallite size of 2 nm. With increasing temperature, the lines are getting sharper as the crystallite size grows to 25 nm at 800 °C, when the transformation to rutile is initialized [18, 19].

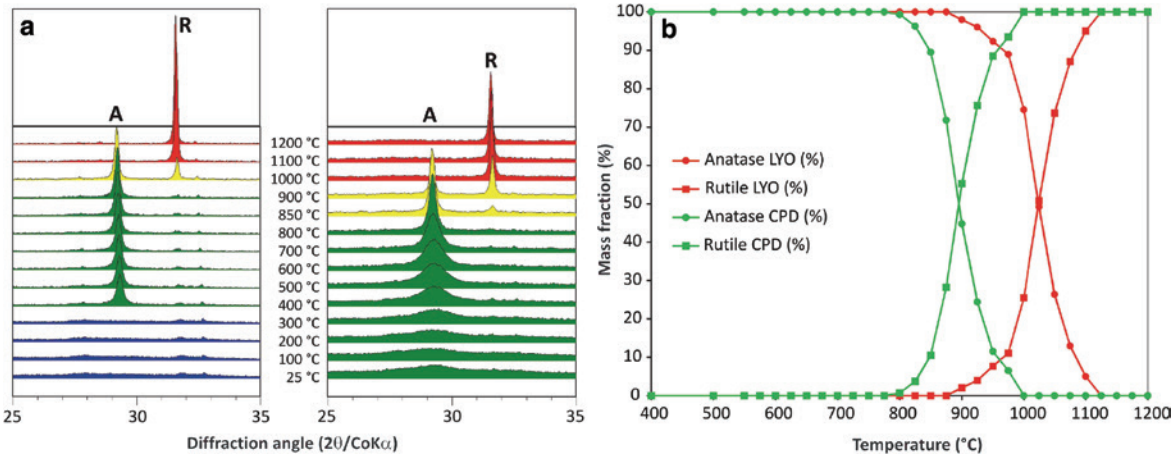

Fig. 3: *In situ* HT XRD analysis of (a) lyophilized (left) and critical point dried (right) and (b) mass fraction of crystalline phases upon heating of titania aerogels.

It is well known that anatase → rutile phase transformation depends significantly on the preparation method, it was reported that the transformation begins above ~ 600 °C, mostly close to this temperature [20]. Nevertheless, this transformation in both samples begins at much higher temperature, and 50 % of the transformation proceeds between 850 and 1100 °C (Fig. 3b). It is well known that bulk rutile is more thermodynamically stable than anatase at all temperatures and pressures owing to its lower free energy. However, the lower surface energy of the anatase planes relative to those of rutile cause the former to be more stable for crystallites of extremely small sizes and correspondingly high surface areas. Further, the size above which rutile becomes more stable depends on stress [20]. Thus we can well understand the high anatase stability in both samples owing to very small average crystallite size of anatase lying in the region of tens of nanometers. The transformation temperature to rutile is significantly lower for the CPD sample by about 100 °C.

The above described differences are likely to be associated with different morphology of the samples. Whereas in the LYO sample with a typical laminar morphology the mass transport is limited and does not allow growth of anatase crystals, the bulk morphology of the CPD sample creates more favorable conditions for mass transfer and thus the growth of crystals.

The FTIR spectra of both prepared titania aerogels are very similar (Fig. 4a). The analysis shows that the samples evidently contain OH^- groups (characteristic bands at 3400 cm^{-1} and at 1600 cm^{-1}), NH_4^+ (at 3200 cm^{-1} and at 1400 cm^{-1}) and peroxogroups (920 cm^{-1}). None of the bands characteristic to sulfates can be observed at 1200 cm^{-1}, which means that the initial $TiOSO_4 \cdot nH_2O$ was decomposed and all sulfur was removed during the synthesis.

The analysis of the Raman spectra (Fig. 4b) reveals that both LYO and CPD samples contain spectral features which can be attributed to Ti-peroxygel, anatase or metatitanic acid. Both LYO and CPD clearly differ from anatase or rutile. The spectra of both LYO (especially) and CPD are significantly similar to the spectra of Ti-peroxy gel formed at surface of Ti metal by action of hydrogen peroxide described by Muyco et al. [21]. Both samples, LYO and CPD, contain weak or middle intensity bands with peaks at positions: 197, (198), 299 (shoulder), (286) and 387, (385) cm^{-1}, which correspond to 191, 287.5 and 387 cm^{-1} attributed to Ti-peroxy gel, and bands of LYO (CPD) at 281 (272) and 448 (442) cm^{-1} can be related to 269 and 449 cm^{-1} attributed to titania. The strongest band in LYO (or CPD) at 705 (700), and bands at 823 (821) and 916 (920) cm^{-1} can be considered as analogues to the bands ascribed tentatively to metatitanic acid (H_2TiO_3). Furthermore, in the CPD spectrum, a very strong band at 150 cm^{-1} and less intense bands at 635, 514, and 385 cm^{-1} can be ascribed to anatase Raman active modes. These bands can be considered as a manifestation of nascent anatase crystals formed in the original Ti-peroxy gel matrix under high pressure conditions. The strong band at 150 cm^{-1} (belonging to anatase) is missing in LYO sample since the sample is amorphous up to 300 °C. This is in good agreement with data obtained by TEM and XRD.

The results of the specific surface area and porosity measurements for both, LYO and CPD sample are given in Table 1. According to the pore size LYO sample is mesoporous and in CPD sample pores are predominantly mesoporous with a small portion of micropores and macropores. CPD sample has more than three times higher specific surface area in comparison with LYO sample. Also the total pore volume is much higher

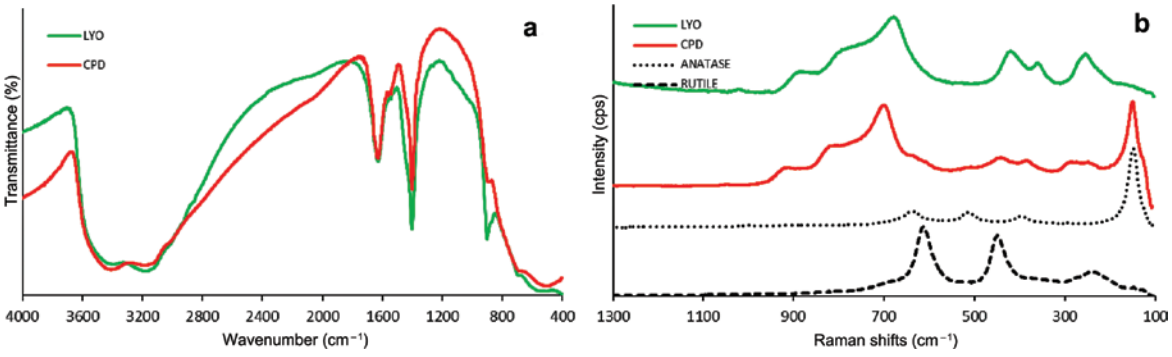

Fig. 4: Comparison of infrared (a) and Raman (b) spectra of lyophilized and critical point dried titania aerogels.

Table 1: Results of the surface area and porosity measurements.

Sample	Surface are ($m^2\ g^{-1}$)	Total pore volume ($cm^3\ g^{-1}$)	Average pore diameter (nm)
LYO	126	0.28	3.1
CPD	392	0.53	3.7

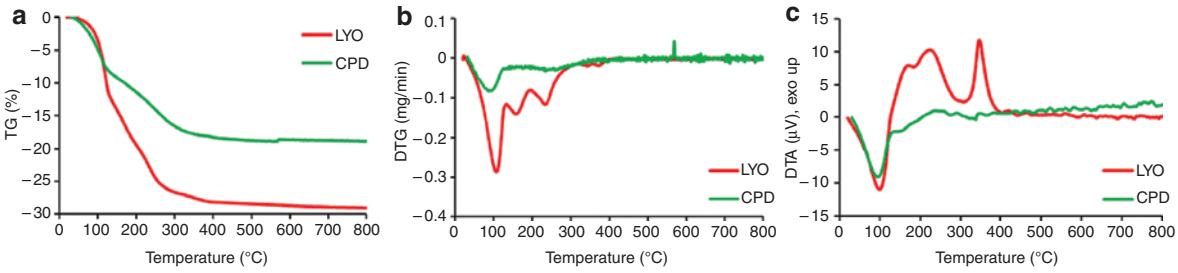

Fig. 5: Comparison of TG (a), DTG (b) and DTA (c) of lyophilized and critical point dried titania aerogels (heating rate 5 °C min^{-1}).

in the CPD sample. The pore diameter between 3 and 4 nm ranks the substances among typical nanoporous aerogels. The measurements presented in Table 1 are in good agreement with the results of SEM and TEM observations (Figs. 1 and 2). Compact foils with flat surface of LYO samples exhibit lower surface area and total pore volume than the bulk material composed of porous 3D network of anatase nanocrystals forming the CPD sample.

In order to compare the thermal decomposition of prepared materials, the thermoanalytical measurements were performed (Fig. 5). The analysis of thermal decomposition of prepared titania aerogels showed that four reaction steps can be distinguished at the LYO material and two reaction steps can be distinguished at the CPD material, by combining information from TG and DTA measurements. The total mass loss is approximately 30 % for LYO and 20 % for CPD material, the main difference is likely the different amount of water in the sample. At the DTA curve of LYO, crystallization of amorphous phase into anatase can be observed which is in good agreement with XRD data. Since the CPD material is crystalline from the beginning, no crystallization can be observed on the DTA curve.

Conclusions

Yellow aqueous colloids of peroxopolytitanic acid can be transferred by lyophilization as well as by critical point drying into yellow highly porous nanostructured aerogels. Products of both types of drying exhibit lamellar morphology with significant differences. Lyophilization results in products consisting of very thin leaves with flat surface, while CPD provides rather bulk highly porous samples with less pronounced foil morphology. In accordance with this finding are significantly higher values of surface area and total pore volume found for the CPD sample. While the lyophilized sample is predominantly amorphous, the CPD dried sample contains significant content of nanocrystalline anatase phase even at room temperature. Upon heating, the CPD sample crystallizes continuously from the room temperature, while the lyophilized sample transforms to anatase suddenly at ~350 °C. However, the anatase crystallites in the lyophilized sample do not grow significantly with rising temperature until the transformation to rutile, whereas in the CPD sample the size of anatase crystallites increases continuously. Such behavior could be explained by the different morphology of the samples. In the lyophilized sample with a typical laminar morphology the mass transport is limited and does not allow growth of anatase crystals. The bulk morphology of the CPD sample, on the other hand, creates more favorable conditions for mass transfer and thus the growth of crystals.

Acknowledgement: The authors acknowledge the assistance provided by the Research Infrastructure NanoEnviCz, supported by the Ministry of Education, Youth and Sports of the Czech Republic under Project No. LM2015073.

References

[1] N. Husing, U. Schubert. *Angewandte Chemie-Int. Edn.* **37**, 23 (1998).
[2] A. Freytag, S. Sánchez-Paradinas, S. Naskar, N. Wendt, M. Colombo, G. Pugliese, J. Poppe, C. Demirci, I. Kretschmer, D. W. Bahnemann, P. Behrens, N. C. Bigall. *Angewandte Chemie Int. Edn.* **55**, 1200 (2016).
[3] J. Subrt, P. Pulisova, J. Bohacek, P. Bezdicka, E. Plizingrova, L. Volfova, J. Kupcik. *Mater. Res. Bull.* **49**, 405 (2014).
[4] S. S. Kistler. *Nature* **127**, 741 (1931).
[5] J. M. van Bemmelen. *Z. Anorg. Chem.* **30**, 265 (1902).
[6] L. Qian, H. F. Zhang. *J. Chem. Technol. Biotechnol.* **86**, 172 (2011).
[7] J. Muhlebach, K. Muller, G. Schwarzenbach. *Inorg. Chem.* **9**, 2381 (1970).
[8] K. Jiang, A. Zakutayev, J. Stowers, M. D. Anderson, J. Tate, D. H. McIntyre, D. C. Johnson, D. A. Keszler. *Solid State Sci.* **11**, 1692 (2009).
[9] E. Plizingrova, L. Volfova, P. Svora, N. K. Labhsetwar, M. Klementova, L. Szatmary, J. Subrt. *Catal Today* **240**, 107 (2015).
[10] M. Sajfrtova, M. Cerhova, V. Drinek, S. Danis, L. Matejova. *J. Supercrit. Fluids* **117**, 289 (2016).
[11] J. L. Labar. *Ultramicroscopy* **103**, 237 (2005).
[12] *JCPDS PDF-4 Database, International Centre for Diffraction Data, Newtown Square, PA, U.S.A. release 2016.*
[13] *NICODOM Raman Library, 5118 spectra, NICODOM Ltd., Hlavni 2727, CZ-14100 Praha 4, Czech Republic, EU.*
[14] S. Brunauer, P. H. Emmett, E. Teller. *J Am Chem Soc* **60**, 309 (1938).
[15] E. P. Barrett, L. G. Joyner, P. P. Halenda. *J Am Chem Soc* **73**, 373 (1951).
[16] E. Pližingrová, M. Klementová, P. Bezdička, J. Boháček, Z. Barbieriková, D. Dvoranová, M. Mazúr, J. Krýsa, J. Šubrt, V. Brezová. *Catalysis Today*, DOI:10.1016/j.cattod.2016.08.013.
[17] D. Schwarzenbach. *Inorg. Chem.* **9**, 2391 (1970).
[18] Y. J. Sun, T. Egawa, L. Y. Zhang, X. Yao. *Jpn. J. Appl. Phys. Part 2-Lett.* **41**, L945 (2002).
[19] R. D. Shannon, J. A. Pask. *J. Am. Ceram. Soc.* **48**, 391 (1965).
[20] D. A. H. Hanaor, C. C. Sorrell. *J. Mater. Sci.* **46**, 855 (2011).
[21] J. J. Muyco, J. J. Gray, T. V. Ratto, C. A. Orme, J. McKittrick, J. Frangos. *Mater. Sci. Eng. C-Biomimetic Supramol. Syst.* **26**, 1408 (2006).